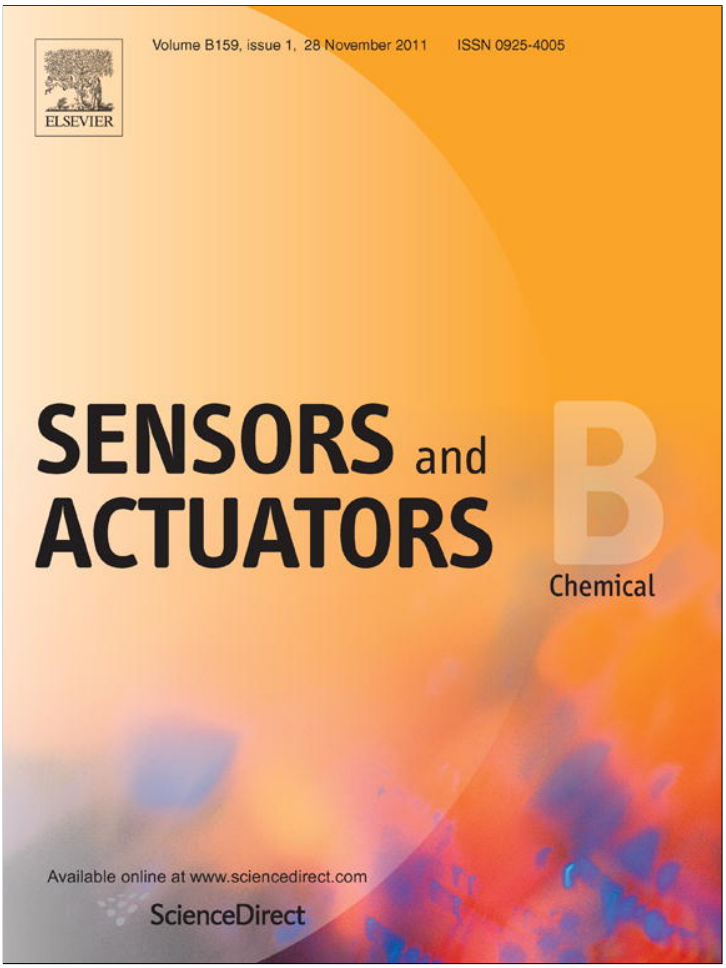

Sensors and Actuators B 159 (2011) 261–270

Contents lists available at ScienceDirect

Sensors and Actuators B: Chemical

journal homepage: www.elsevier.com/locate/snb

Screen-printed carbon electrode for choline based on MnO_2 nanoparticles and choline oxidase/polyelectrolyte layers

E.A. Dontsova[a], Y.S. Zeifman[a], I.A. Budashov[b], A.V. Eremenko[c], S.L. Kalnov[b], I.N. Kurochkin[a,*]

[a] Department of Chemistry, M.V. Lomonosov Moscow State University, Leninskie gory 1/3, 119991 Moscow, Russia
[b] Emanuel Institute of Biochemical Physics of Russian Academy of Sciences, Kosygina 4, 119991 Moscow, Russia
[c] A.N. Belozersky Institute of Physico-Chemical Biology, Moscow State University, Leninskie gory 1/40, 119991 Moscow, Russia

ARTICLE INFO

Article history:
Received 17 November 2010
Received in revised form 28 June 2011
Accepted 1 July 2011
Available online 7 July 2011

Keywords:
Choline biosensor
Layer-by-layer assembly
Manganese dioxide nanoparticles mediating layer
Screen-printed carbon electrode

ABSTRACT

This paper presents the amperometric biosensor that determines choline and cholinesterase activity using a screen printed graphite electrode. In order to detect H_2O_2 we have blanket modified the electrode material with manganese dioxide nanoparticles layer. Using layer-by-layer technique on the developed hydrogen peroxide sensitive electrode surface choline oxidase was incorporated into the interpolyelectrolyte nanofilm. Its ability to serve as a detector of choline in bulk analysis and cholinesterase assay was investigated. We examined the interferences from red-ox species and heavy metals in the blood and in the environmental sample matrixes. The sensor exhibited a linear increase of the amperometric signal at the concentration of choline ranging from 1.3×10^{-7} to 1.0×10^{-4} M, with a detection limit (evaluated as 3σ) of 130 nM and a sensitivity of 103 mA M^{-1} cm^{-2} under optimized potential applied (480 mV vs. Ag/AgCl). The biosensor retained its activity for more than 10 consecutive measurements and kept 75% of initial activity for three weeks of storage at 4 °C. The R.S.D. was determined as 1.9% for a choline concentration of 10^{-4} M ($n = 10$) with a typical response time of about 10 s. The developed choline biosensor was applied for butyrylcholinesterase assay showing a detection limit of 5 pM (3σ). We used the biosensor to develop the cholinesterase inhibitor assay. Detection limit for chlorpyrifos was estimated as 50 pM.

1. Introduction

Cholinesterases have important physiological functions: acetylcholinesterase (AChE) is involved in neural signal transduction catalyzing hydrolysis of neurotransmitter acetylcholine [1,2], butyrylcholinesterase (BChE) act as stoichiometric scavenger of organophosphates [3,4]. These enzymes can be inhibited by pesticides. Currently, activities of blood esterases and concentrations of their inhibitors are determined by using techniques for registration of 'exogenous' choline generated by biocatalytic hydrolysis of choline esters. The application of modern electrochemical biosensors is a good alternative to routinely used methods due to high sensitivity achieved in recent years.

Thus significance of 'exogenous' choline has attracted much interest in developing simple and fast analytical methods for selective monitoring of the cholinesterase inhibitors, as well as the prompt analysis of blood esterase activities in surveillance of individuals, exposed to cholinergic and neuropathic organophosphorus compounds [5].

Enzyme based amperometric biosensors are traditionally used for a reliable and rapid detection of choline in aqueous medium. The biosensor detection of choline is based on its biocatalytic oxidation by choline oxidase, immobilized on the electrode surface generating hydrogen peroxide. The following registration of hydrogen peroxide can be achieved by direct, mediated and horseradish peroxidase containing electrodes [6]. The recent application of mediating layers in hydrogen peroxide sensing electrodes fabrication resulted in the lowest hydrogen peroxide detection limits ranging from 4 to 60 nM [7]. Previous work on the mediator based biosensors containing hydrogen peroxide sensitive layers focused on the metal–organic complexes of Ni^{2+} [8], Cu^{2+} [9], Fe^{3+} (ferrocene) [10] and Co^{2+} (phthalocyanine) [11], complexes of transition metals and polymers (Os^{3+}) [12], Prussian blue [13–16], oxides of cobalt [17,18], manganese [7,19–22] iridium [23] and vanadium [24]. Most of the mentioned above devices used electrochemical/chemical deposition for mediator layer fabrication [20,25]. Several methods for choline oxidase immobilization on a surface of electrochemical sensors included covalent immobilization [26–28], incorporation into membrane pores [29] and electropolymerized films [30,31], cross-linking immobilization in thick films [15] and, a more recent, layer-by-layer (LBL) method [25,32,33]. In general, the modified electrodes showed improved electrocatalytic responses with reduced overpotentials and

* Corresponding author. Tel.: +7 939 43 91; fax: +7 939 40 42.
E-mail address: ikur@genebee.msu.su (I.N. Kurochkin).

0925-4005/$ – see front matter © 2011 Elsevier B.V. All rights reserved.
doi:10.1016/j.snb.2011.07.001

increased voltammetric signals allowing low detection limits and high sensitivities.

The problem is that the proposed immobilization techniques for the deposition of hydrogen peroxide oxidation mediating layers and choline oxidase are hard and time-consuming to reproduce, have poor enzyme activity, and insufficient spatially controlled deposition. These disadvantages led to the development of the new technological approach to the electrochemical biosensors. This approach focuses on immobilization technique of the main sensor components: enzymes and mediators. More specifically, our automatic methods are based on mechanical plotting of small liquid volumes. One of them, the ink-jet printing, is accurate, simple for control and applicable for wide range of sensor surfaces [34]. The ink-jet printing requires the development of a special composite water-based material, containing the panel of desired nanosized components for immobilization. Previous research [21] showed that MnO_2 nanoparticles have special physical and chemical properties, that are different from common MnO_2 powders. On the one hand, they provide significant improvement of mediating properties, on the other hand, they simplify the stable water and organic mixtures. For example, MnO_2 nanoparticles can be homogeneously dispersed in water colloidal Na-montmorillonite solution [22] or reversed micellar solution of MnO_2 nanoparticles can be prepared in hexane [7]. In both cases their properties assist at the preparation of the stable and uniform hydrogen peroxide oxidation mediating layers. These layers are more permeable and conductive than Nafion films, which are commonly used to modify electrodes. The process of preparation of hydrogen peroxide mediating layers based on MnO_2 nanoparticles can be simplified and improved by depletion of additional stabilizers from colloidal mixtures: Na-montmorillonite or organic solvents.

Researchers have investigated mediator properties of amorphous, α-phase and β-phase modifications of MnO_2 nanoparticles developed for H_2O_2 and choline [31,35,36]. The results showed that MnO_2 can be applied as a mediator for the oxidative [31] and reducing [31,35,36] H_2O_2 decomposition. They reached low detections limits for choline (1.0 μM and 0.3 μM, respectively) having reduced the decomposition of H_2O_2 on glassy carbon electrode, modified with α-phase and β-phase MnO_2. Further, the room temperature synthesis is known to result in the production of a highly catalytically active gamma-phase MnO_2 [37]. However, there was no data on the appropriate mediator properties of γ-phase MnO_2 for H_2O_2 and choline detection.

The present research investigates red-ox mediator properties of gamma-phase MnO_2 produced at the room temperature in water solution for the biosensor application. This paper introduces the screen-printed amperometric sensor based on aqueous γ-phase-MnO_2 as hydrogen peroxide oxidation mediating reagent. Further, we focus on the electrostatic assembly of a choline oxidase on the interpolyelectrolyte nanofilm. The proposed approach for the biosensor manufacturing is technological and highly productive. At the same time, it achieves an excellent sensitive measurement of choline, butyrylcholinesterase and its inhibitors.

2. Experimental sections

2.1. Materials

We have used potassium permanganate (Chimmed, Russia) and manganese acetate tetra hydrate (Acros, Belgium) for manganese dioxide sol solutions preparation. Choline oxidase (ChOx) (from *Alcaligenes sp.*, E.C. 1.1.3.17, 11.6 U mg^{-1}) was obtained from Fluka (Germany). Butyrylcholinesterase (BChE) (from equine serum, E.C. 3.1.1.8, 264 U mg^{-1}), (4-(2-hydroxyethyl)-1-piperazineethanesulfonic acid), (Hepes), choline was obtained from Sigma (USA). Hydrogen peroxide (30%, w/w water solution) was purchased from Merck (Germany), bovine serum albumin (BSA) was obtained from Serva (USA). Polydimethyldiallyl ammonium chloride (PDDA) (20%, w/w water solution) (Sigma–Aldrich, Germany) and sodium polyanethol sulfonate (PAS) (Serva, USA) were used for sensor preparation. Butyrylcholine chloride was obtained from the organic synthesis group of Chemical Enzymology Division of the MSU (Russia). All other reagents (ascorbic and uric acids and inorganic salts) were of analytical grade. All solutions were prepared with doubly distilled water.

2.2. Apparatus

Transmission electron microscopy (TEM, LEO912 AB OMEGA), spectrophotometry (spectrophotometer Carry-100) and quasi-elastic dynamic scattering (ALV DLS/SLS-SP 5022F, He–Ne laser of goniometer ALV-SP 125 with wave-length 632.8 nm, correlator ALV 5000/E) were used to characterize MnO_2 sol solutions. In order to characterize the surface of screen-printed electrodes we have utilized the scanning electron microscopy (SEM, Carl Zeiss Supra 40). A potentiostate IPC-2000 (Kronas Ltd., Russia) was used for electrochemical measurements.

2.3. Preparation and characterization of MnO_2 sol solutions

We have obtained manganese dioxide sol solutions by mixing diluted water solutions of manganese (II) acetate and potassium permanganate. The choice of manganese acetate and potassium permanganate concentrations in the initial solutions was based on the stoichiometric ratio of the reagents in the reaction:

$$3(CH_3COO)_2Mn{\cdot}4H_2O + 2KMnO_4 \rightarrow 5MnO_2 + 2CH_3COOK + 4CH_3COOH + 2H_2O$$

The concentration range for $KMnO_4$ was 0.01–0.5 mM and for $Mn(Ac)_2$ 0.015–0.75 mM subsequently. The optimal concentrations obtained for $KMnO_4$ and $Mn(Ac)_2$ were 0.25 mM and 0.375 mM, consequently. Reagent solutions were mixed (0.5 ml of each reagent) and shaken for 5 min. A freshly prepared MnO_2 solution was used for the sensor preparation. The optical density (OD) (at λ = 366 nm) characterizes the corresponding MnO_2 concentration in obtained sols. OD was measured with microplate spectrophotometer xMark (Bio-rad, USA).

To obtain TEM images of MnO_2, 5 μl drop of MnO_2 sol solution with OD = 1.6 was dried on the surface of the cupper grid (200 mesh, Pelco, USA) with the support film of formvar stabilized with the carbon at a room temperature, then it was rinsed with the bidistilled water and dried. For spectrophotometric studies we have utilized MnO_2 sol solution with estimated OD = 0.8. For quasi-elastic dynamic scattering we have filtered the initial $KMnO_4$ and $Mn(Ac)_2$ solutions through a 0.2 μm porous membrane three times. To obtain scanning electron microscopy (SEM) surface images of layers formed with developed manganese dioxide nanoparticles, a drop of MnO_2 sol solution (OD = 1.6) was dried on the surface of freshly split high oriented pirrolytic graphite (HOPG) (NT-MDT, Russia) or screen-printed carbon electrode, rinsed with bidistilled water and dried.

The measurements of ζ-potential of manganese dioxide nanoparticles were carried out on a Malvern Zetasizer Nano-ZS (Malvern Instruments, UK). Before measurement the MnO_2 sol solutions (OD = 1.6) were diluted in 20 times with bidistilled water.

2.4. Fabrication of biosensors

Screen-printed carbon electrodes (SPE) were made using semi-automated machine Winon (model WSC-160B, China) with 200

mesh screen stencil. Polyvinyl chloride substrate of 0.2 mm thickness and conductive graphite paste (Coates Screen, Germany) was used. Each SPE consisted of a round-shaped working area (3 mm diameter), a conductive track (30 mm × 1.5 mm), and a square extremity (3 mm × 7 mm) for the electrical contact.

Peroxide-sensitive layer was formed by dropping 5 μl of MnO_2 sol solution on the working area of the electrode followed by drying at a room temperature for 40 min. Then the electrode was rinsed with bidistilled water and dried at a temperature of 60 °C for 1 h. Linear voltammograms of electrodes were measured from 250 mV to +750 mV with scan rate 20 mV s^{-1}.

We have used MnO_2-modified SPE in order to make choline oxidase sensors according to the following procedure. Choline oxidase was dissolved in 50 mM Hepes buffer, containing 30 mM KCl (pH 7.5). Polyelectrolytes (PDDA and PAS) were dissolved in bidistilled water at concentration 5 mg ml^{-1}. For preparation of PDDA/ChOx nanofilms, a 5 μl drop of PDDA solution was put on the surface of MnO_2-modified electrodes and in 10 min (before the drop dried) the electrodes were rinsed with bidistilled water for 1–2 min. The electrodes were then dried and a 5 μl drop of ChOx solution was put on the electrodes' surface (the optimal concentration of ChOx in the solution was estimated as 0.5 mg/ml). After 10 min of adsorption, the electrodes were rinsed with water and dried. The same procedure was used to prepare complex nanofilms containing several interpolyelectrolyte layers $(PDDA/PAS)_2$ and several enzyme/polyelectrolyte layers $(PDDA/ChOx)_n$ on the electrode surfaces.

2.5. Electrochemical measurements

Amperometric measurements were performed with IPC-2000 at room temperature in 1 ml electrochemical cell with magnetic stirrer in 50 mM Hepes buffer (30 mM KCl, pH 7.0–8.2). We have employed a two-electrode configuration that consisted of a screen-printed carbon modified (3 mm diameter) electrode serving as a working electrode and Ag/AgCl reference electrode. A working potential in the range of 150–550 mV (vs. Ag/AgCl reference electrode) was applied to the electrode. Analytical response constituted a difference between the current in the presence and the absence of hydrogen peroxide or choline.

2.6. Butyrylcholinesterase assay

We have utilized the following two approaches to conduct butyrylcholinesterase (BChE) assay. To determine the BChE activity in spike-solutions of mice blood haemolysates (kindly provided by Institute of Physiologically Active Compounds RAS), by 'end point' variant, the BChE solutions (0.5–2.5 nM) were prepared in 50 mM Hepes buffer (30 mM KCl, 1 mg ml^{-1} BSA, pH 7.5). We have initiated the reaction by addition of butyrylcholine (final concentration 10 mM) to mixture, containing 20 μl of haemolysate and 20 μl of BChE solution. After 30 min incubation at room temperature choline concentration was measured using amperometric biosensor.

The estimation of BChE activity by kinetic method was conducted in the mentioned above Hepes buffer, using amperometric biosensor at butyrylcholine final concentration 1.8 mM. In this case the analytical response was proportional to the rate of choline generation. The rate of the non-enzymatic hydrolysis was validated by the analytical response in the absence of the enzyme.

2.7. Choline esterases inhibitor assay

Chlorpyrifos after 10 min oxidation by 'bromide water' (0.1% Br_2 in 0.5 M KBr solution) at room temperature was used as an inhibitor in choline esterases inhibitor assay. We have used the following SPE in the inhibitor analysis: $MnO_2/(PDDA/PAS)_2/(PDDA/ChOx)_3$. We performed the analysis by measuring the degree of inhibition (i.e. ratio of BChE activity after 10 min incubation with chlorpyrifos to enzyme activity without inhibitor).

3. Results and discussion

In the process of assembling screen-printed choline oxidase – based electrodes we have performed several optimizations to obtain a reliable composite sensor surface containing: (a) hydrogen peroxide sensitive layer based on MnO_2 nanoparticles, and (b) layer-by-layer assembled enzyme and polyelectrolyte.

3.1. Synthesis, stabilization and characterization of MnO_2 nanoparticles

For synthesis of MnO_2 nanoparticles a comproportionation reaction (using $KMnO_4$ as the oxidant and Mn^{2+} salts as reducing agent) in aqueous solutions at ambient temperature was applied. The reaction leads to formation of manganese dioxide nanoparticles reddish brown dispersion in dilute solutions. These nanoparticles in water solution present typical colloidal system that is are called hydrosol. The stability of the MnO_2 hydrosol is crucial for assembling a hydrogen peroxide sensitive layer onto the electrode surface. The addition of various ions (capable to complete a crystal lattice or at least to be adsorbed on a surface of a crystal phase) to the colloidal system allows the stabilization of hydrosols and the prevention of the particles' aggregation. One of the commonly used methods is the stabilization of hydrosols by controlling the surface charge properties of the nanoparticles using different anions.

The interaction of $KMnO_4$ with manganese (II) chloride resulted in rapid coagulation of sol forming a pellet. We have observed the same effect in the presence of sulfate, dodecylsulphate, fluoride, and carbonate ions. However, acetate, hydrocarbonate, hydro- and dihydrophosphate ions are promoted stabilization and formed manganese dioxide hydrosol. Moreover, stable (for several weeks) manganese dioxide hydrosol was obtained during the introduction into the reaction of manganese (II) acetate instead of manganese chloride. The images of manganese dioxide hydrosol preparations (Fig. 1) obtained using manganese chloride (Fig. 1(a)) and manganese acetate (Fig. 1(b)) reflect sedimentation and stable colloidal solution subsequently. We propose that the stabilization of nanoparticles using manganese acetate is provided by a high degree of acetate-ion hydration in accordance with Hofmeister series [38]. Thus, in the presence of acetate charge screen on the particles surface is lowered, protecting them from aggregation.

According to TEM data, most of chloride-based MnO_2 nanoparticles represent aggregates with dimensions from deciles of microns to several microns. Acetate-based MnO_2 nanoparticles represent wrinkled lamellar structures with estimated thickness 0.3–0.6 nm and characteristic dimensions 50–120 nm. The particles have polycrystalline nature; the crystalline sizes are about 2 nm. We have obtained electron energy loss spectrum with TEM (Fig. 1(c)). The peaks observed at 645 eV and 655 eV corresponded to manganese (according to TEM database).

The crystal phase of the MnO_2 was analyzed by powder X-ray diffraction. The diffraction peaks can be indexed to orthorhombic symmetry and corresponding to γ-MnO_2 (ICDD –JCPDS Card No. 72-1983).

Fig. 2 presents spectrophotometrical data for hydrosol (Fig. 2). The absorption peak at 366 nm confirmed, that hydrosol contained MnO_2 [39]. The hydrodynamic radius of manganese dioxide nanoparticles, estimated via light scattering, was 64 ± 1 nm. Fig. 3(a) shows the SEM image of hydrosol dried on HOPG surface. The dimensions of separate particles are about 60–100 nm.

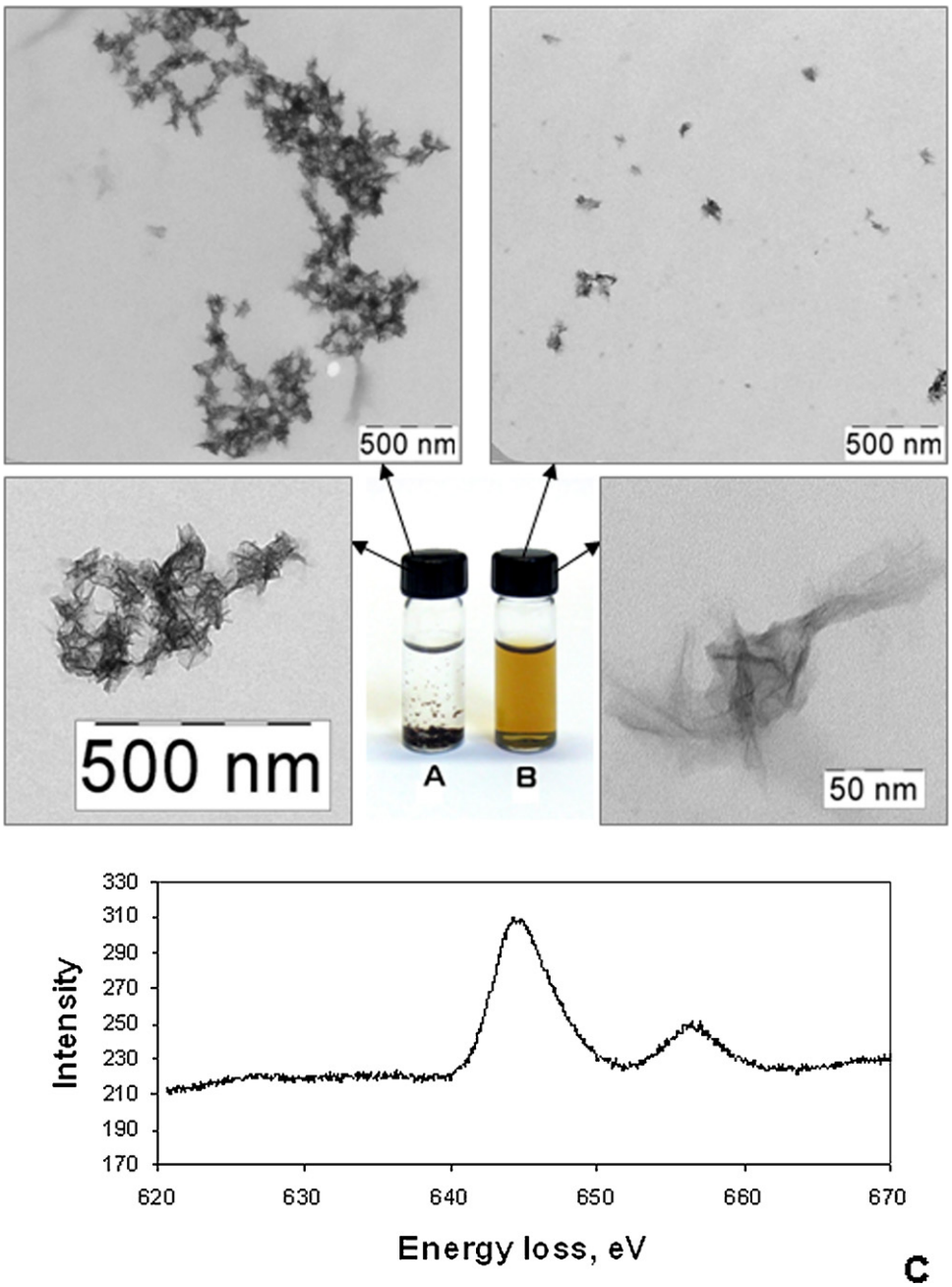

Fig. 1. Photographs and TEM images of different colloidal MnO_2 particles obtained in water according to comproportionation of potassium permanganate (0.250 mM) and (a) manganese (II) chloride (0.375 mM), (b) manganese (II) acetate (0.375 mM) resting for 14 days. (c) Electron energy loss spectrum for manganese dioxide sol solutions obtained in acetate.

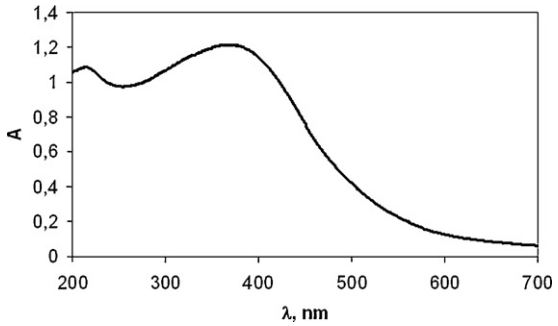

Fig. 2. Absorption spectra of MnO_2 sol solution.

The measurement of ζ-potential for acetate-based manganese dioxide nanoparticles in hydrosol estimated −30 mV. In a lyotropic series of monovalent cations the increase of ionic radius (decrease of hydration of an ion) led to the decrease of the coagulation threshold (within 24 h of the observation after the addition of the electrolyte):

$$Li^{+}(12.0\,mM) > Na^{+}(8.0\,mM) > K^{+}(5.0\,mM) > Rb^{+}(4.5\,mM) > Cs^{+}(4.0\,mM)$$

Similar trend was observed for bivalent cations: $Mg^{2+}(0.30\,mM) > Ca^{2+}(0.20\,mM) > Ba^{2+}(0.15\,mM)$.

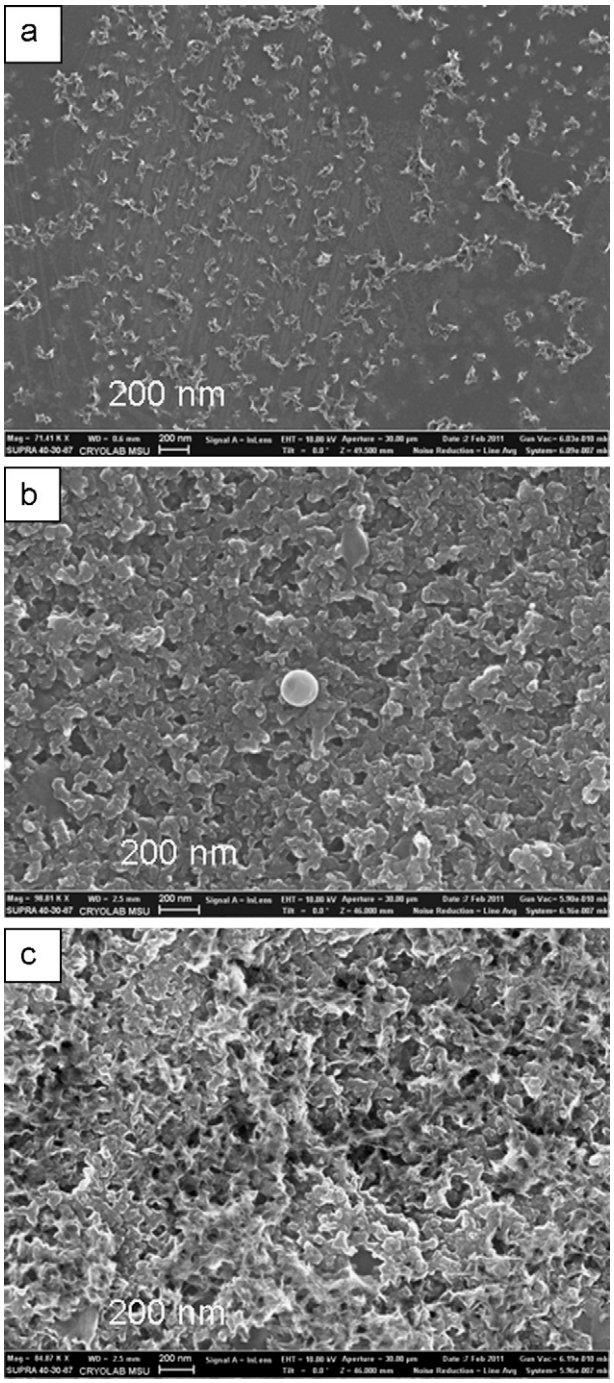

Fig. 3. SEM image of MnO_2 nanoparticles on the surface of HOPG (a) and SEM images of SPE unmodified (b) and modified with MnO_2 nanoparticles (c).

Thus, the above mentioned stable manganese dioxide hydrosol was obtained in the reaction of reduction of potassium permanganate by bivalent manganese in the presence of acetate-ions.

3.2. Electrochemical studies of MnO_2-modified SPE

Fig. 3 shows the SEM image of unmodified (b) and modified by MnO_2 nanoparticles (c) SPE surface. Nanoparticles with characteristic "wrinkled" structure cover a part of the demonstrated electrode surface (Fig. 3(c)).

Electrochemical characteristics of SPE covered with manganese dioxide have been studied. Fig. 4 illustrates linear voltammograms obtained with the MnO_2-modified (a and b) and unmodified (c and d) SPE in the absence (b and d) and presence of 0.1 mM H_2O_2 (a and c) in 50 mM Hepes buffer, pH 7.5, 30 mM KCl. The image shows the increase of the current in the presence of modified electrode due to the oxidation of Mn (II, III) to MnO_2 in accordance with [22]. The voltammogram obtained in the presence of hydrogen peroxide showed higher levels of oxidation current in comparison with similar data obtained in Hepes buffer. In this case the oxidation of hydrogen peroxide resulted in the reduction of MnO_2 and the formation of Mn (II) and (III) oxides. It further led to the oxidation of these oxides with reiterated generation of MnO_2 on the electrode surface [20,22]. Fig. 4(e) shows the difference voltammogram, obtained by subtraction of voltammogram without H_2O_2 (Fig. 4b) from voltammogram with H_2O_2 (Fig. 4a). There is an evident peak, corresponding to H_2O_2 oxidation at 600 mV.

Table 1
Long-term stability of peroxide-sensitive electrodes. Measurement conditions: 50 mM Hepes, pH 7.5, 30 mM KCl, 250 mV vs. Ag/AgCl, 10 μM H_2O_2. I_0, response of MnO_2-modified sensor to H_2O_2, day 0 (zero).

Days of storage	$\Delta I/\Delta I_0$
0	1.00
7	1.14
14	0.98
21	1.22
28	0.97
35	1.11
42	1.15
49	1.23
56	0.98

Fig. 5(a) presents the response of MnO_2-modified electrode to hydrogen peroxide. The electrode response appeared within the first several seconds (it took 6 s to reach 90% of the final response).

Fig. 5(b) shows the dependence of amperometric electrode response to 10 μM H_2O_2 at different working potential range varying from 150 mV to 550 mV. The analytical response is rising up to 250 mV and then reaches the saturation level. There is a sharp increase in the background current without hydrogen peroxide after 500 mV that may lead to a less accurate measurement of the specific electrode response. Therefore, the optimal range of potentials for further H_2O_2 measurements was determined between 250 mV and 500 mV.

The expected electrode response to hydrogen peroxide depended on the MnO_2 concentration. Fig. 6 reflects the correlation of manganese dioxide sol OD (λ = 366 nm) and the electrode response at hydrogen peroxide concentration 1 μM. It also shows that the analytical response does not change after OD = 1.6.

Fig. 7 shows the calibration curves for hydrogen peroxide obtained at working potential of 250 mV (A) and 480 mV (B), respectively. In both cases, there is a linear increase of the electrode response over the entire range of examined H_2O_2 concentrations. We have calculated the detection limit (45 nM M (3σ)) at 250 mV according to the equation: $y = 23.6x - 0.3$, where y represents the current in nA and x - the H_2O_2 concentration in μM. The linear range was 4.5×10^{-8}–1.0×10^{-4} M, and the sensitivity was estimated as 377 ± 1 mA M^{-1} cm^{-2}. Similar results were obtained for the potential 480 mV with hydrogen peroxide linear range 2.2×10^{-8}–1.0×10^{-4} M. We have estimated the detection limit (22 nM (3σ)) for hydrogen peroxide based on the following equation: $y = 36.1x + 0.1$, with the sensitivity 515 ± 3 mA M^{-1} cm^{-2}. The obtained analytical parameters for hydrogen peroxide amperometric sensors based on MnO_2 have a significant advantage over previously reported ones [7,20,22].

Operational stability of peroxide-sensitive electrodes was investigated at potentials 250 mV and 480 mV, in Hepes buffer (pH 7.5). Ten measurements were performed for each electrode for 10 μM

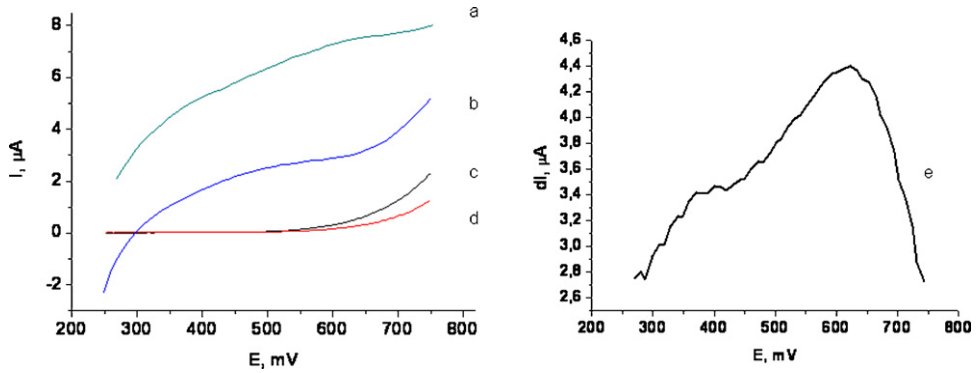

Fig. 4. Voltammograms of SPE: MnO_2-modified (a and b) and unmodified (c and d). Measurement conditions: 50 mM Hepes, pH 7.5, 30 mM KCl, initial potential 0 mV, final potential 650 mV, potential scan rate 20 mV s^{-1}, concentration of H_2O_2 in the electrochemical cell 0 M (b and d) and 0.1 mM (a and c). (e) Difference voltammogram, obtained by subtraction of voltammogram without H_2O_2 (b) from voltammogram with H_2O_2 (a).

H_2O_2 with R.S.D. 5.5 ± 1.7% for 250 mV and 5.0 ± 3.0% for 480 mV. Storing of the MnO_2-modified electrodes at room temperature for two months did not lead to any changes in analytical characteristics of the tested sensors (Table 1).

3.3. Amperometric choline oxidase based biosensor

We have performed the validation of peroxide-sensitive sensors, as a new transducer element based on MnO_2 nanoparticles, for the fabrication of choline oxidase biosensor. Choline oxidase was immobilized on the hydrogen peroxide sensitive electrode surface using "layer-by-layer" technology. The estimated isoelectric point of choline oxidase is 4.1, thus enzyme was negatively charged at its pH optimum (7.0–8.5). Prior to enzyme immobilization, polycation (PDDA) was adsorbed on the surface of MnO_2-modified graphite electrode. Then we have deposited choline oxidase to the same surface (Fig. 8(a)) from an appropriate buffer solution. Fig. 8(c) presents choline detection by amperometric choline oxidase based biosensors.

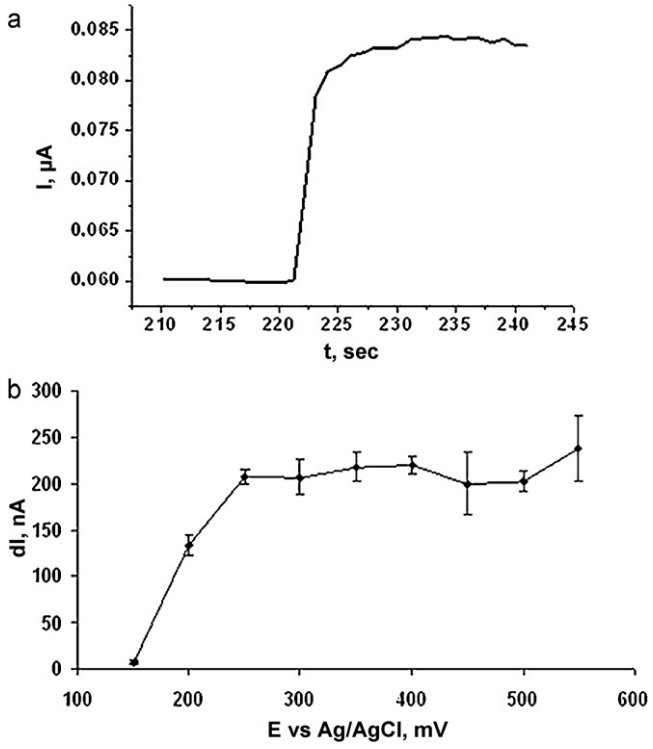

Fig. 5. (a) Anlytical response of MnO_2-modified sensor to 1 μM of H_2O_2, working potential 480 mV vs. Ag/AgCl. (b) Analytical responses of MnO_2-modified electrodes to 10 μM of H_2O_2 under different working potentials vs. Ag/AgCl. Measurement conditions: 50 mM Hepes, 30 mM KCl, pH 7.5.

Table 2
Dependence of analytical response (0.1 mM of choline) and reproducibility of MnO_2/PDDA/ChOx biosensor on choline oxidase concentration. Measurement conditions: 50 mM Hepes, pH 7.5, 30 mM KCl, 480 mV vs. Ag/AgCl.

ChO concentration (mg ml^{-1})	Δ*I* (nA)	R.S.D. % of the response to choline for five different biosensors
0.05	58	16
0.10	98	13
0.50	239	13
1.00	276	24
2.00	318	29
4.00	331	37

First, we evaluated the biosensor response at different concentrations of choline oxidase in solution for adsorption (Table 2). The analytical response increased from 0.05 mg ml^{-1} to 4.00 mg ml^{-1} of choline oxidase concentration in solution for adsorption. R.S.D.% from 5 different electrodes was utilized for validation of sensor fabrication reproducibility. Minimal R.S.D. (13–16%) was observed, when concentration of choline oxidase varied from 0.05 to 0.5 mg ml^{-1}. Thus, the selected optimum of enzyme concentration for effective biosensor functioning was 0.5 mg ml^{-1}.

The investigation of operational stability of the developed choline oxidase biosensors showed that there was a trend for decrease in analytical response from measurement to measurement.

In the selected fabrication scheme MnO_2/PDDA/ChOx, the decrement of sensor analytical response was 2.1 ± 0.1% per one

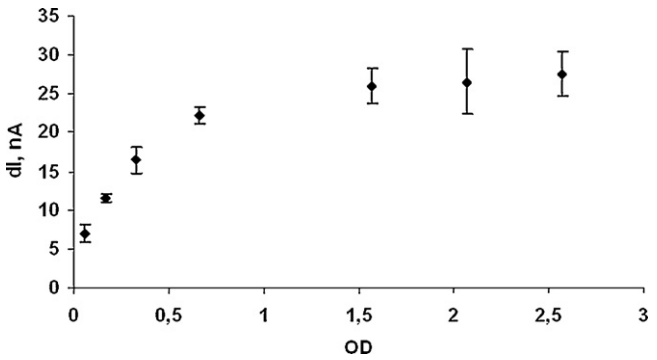

Fig. 6. The correlation between MnO_2 sol solution optical density (λ = 366 nm) and analytical response to H_2O_2 of the obtained peroxide-sensitive layer. Measurement conditions: 50 mM Hepes, pH 7.5, 30 mM KCl, 480 mV vs. Ag/AgCl, 1 μM of H_2O_2.

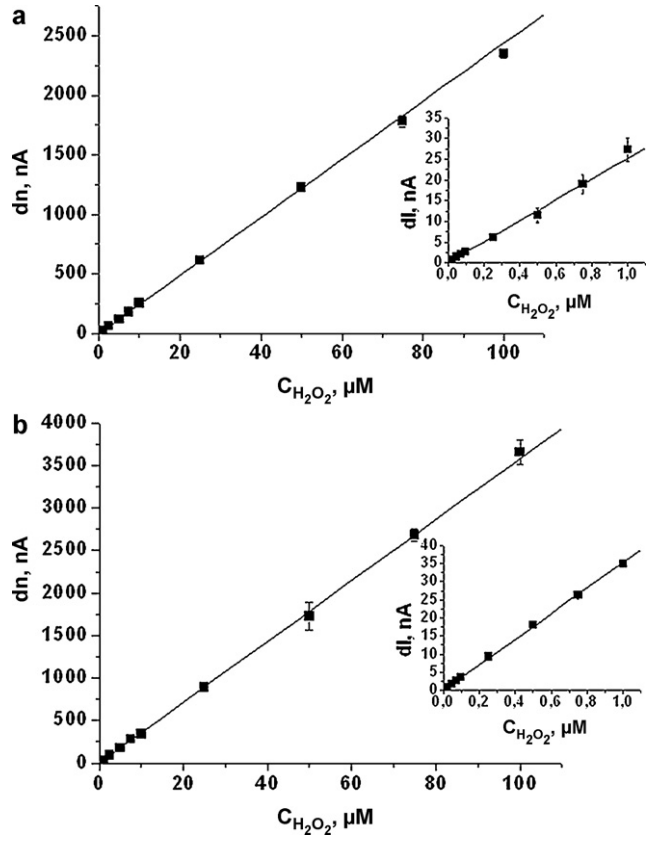

Fig. 7. Calibration plots of MnO_2-modified electrodes for H_2O_2 at 250 mV (a) and 480 mV (b) vs. Ag/AgCl. Measurement conditions: 50 mM Hepes, 30 mM KCl, pH 7.5.

measurement (R.S.D. was 7.0 ± 0.3% per ten measurements) at working potential 480 mV. We have investigated the operation stability of MnO_2 layer at different hydrosol concentrations. Concentrations of MnO_2 in hydrosol were chosen for linear (OD = 0.2) and saturated (OD = 1.6) response–concentration curve areas (Fig. 6) Sensor operation stability was determined in the same ranges of concentrations, i.e. the decrement of analytical response was estimated as 0.2 ± 0.4% (R.S.D. = 2.0 ± 0.1%). All this proves, that

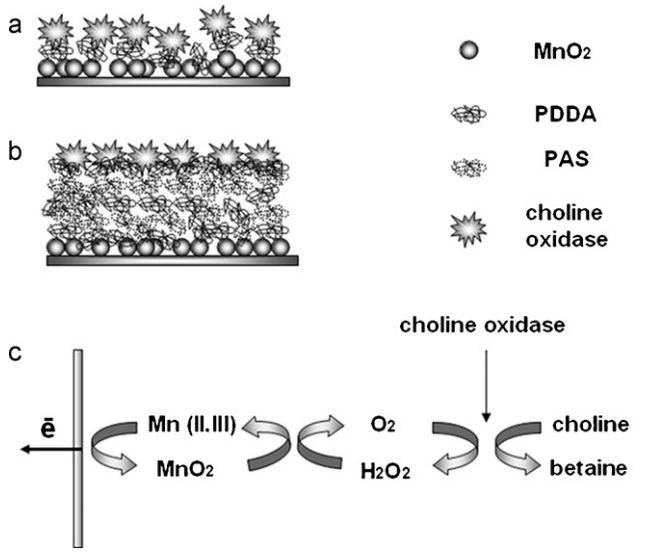

Fig. 8. Architectures of enzyme/polyelectrolyte layers of MnO_2-based choline oxidase biosensor (a) PDDA/ChOx, (b) $(PDDA/PAS)_2$/PDDA/ChOx and (c) scheme of choline detection.

hydrogen peroxide-sensitive layer remained intact. It follows, that the observed decay in the sensor response is connected with the enzyme layer. The improved stabilization of choline oxidase layers was carried out with two additional PDDA/PAS layer's variants (Fig. 8(b)). The decrement of analytical response in this case was 0.6 ± 0.2% (R.S.D. 1.9 ± 0.4%) for $MnO_2/(PDDA/PAS)_2$/PDDA/ChOx electrodes, at working potential 480 mV. At working potential 250 mV the decrement of analytical response for electrodes of the same construction ($MnO_2/(PDDA/PAS)_2$/PDDA/ChOx) was estimated 2.1 ± 0.4% (R.S.D. 9.6 ± 3.0%). These values were 3–5 fold higher than corresponding data obtained for 480 mV. We have selected 480 mV as an optimal for further choline detection.

The increase in the pH dependence values (in the range from 7.0 to 8.2.) led to the increase of the electrochemical response for $MnO_2/(PDDA/PAS)_2$/PDDA/ChOx electrodes. It is known, that pH-optimum of choline oxidase is about 8.0. However, the observed operation stability of choline oxidase biosensors was better at pH 7.5 (decrement of analytical response 0.6 ± 0.2% and R.S.D. = 1.9 ± 0.4%), than at pH 8.2 (decrement of analytical response 3.2 ± 0.0% and R.S.D. = 11.1 ± 0.4%).

We have evaluated storage stability of dried biosensors at 4 °C. Weekly tests showed that the response to 0.1 mM choline of these biosensors kept 75% of initial activity for 3 weeks of storage.

Fig. 9(a) shows a typical steady-state response of choline oxidase biosensor to 0.1 mM of choline. It took about 10 s to reach 90% of the final response.

Fig. 9(b) presents the dependence of choline oxidase biosensor sensitivity on the number of PDDA/ChO layers. The electrode sensitivity increased at magnification of PDDA/ChO layers from 1 to 3, and reached the upper limit.

Fig. 9((c), line I) illustrates the dependence of the $MnO_2/(PDDA/PAS)_2$/PDDA/ChOx sensors responses at the different concentration of choline. Obtained choline calibration curve showed a good linearity in a range between 3.0×10^{-7} and 1.0×10^{-4} M. The corresponding regression equation was: $y = 2.9x + 3.5$, where y represents the current in nA and x the choline concentration in μM. The sensitivity 59 ± 3 mA M^{-1} cm^{-2} and the detection limit 300 nM (3σ) were calculated.

It should be noted, the highest sensitivity of the developed biosensors was obtained during the deposition of three enzyme-containing layers on the electrode surface: $MnO_2/(PDDA/PAS)_2/(PDDA/ChOx)_3$ (Fig. 9(c), line II). In this case the detection limit was 130 nM (3σ) and the sensitivity was 103 ± 3 mA M^{-1} cm^{-2}. These analytical parameters are the best for the amperometric choline oxidase – based biosensors.

The interference of sampling "contaminating" compounds, easily oxidized at positive potentials, is an important factor for evaluating the analytical performance of the electrochemical choline biosensor for medical and environmental applications. We have investigated these potential aberrations, introduced by interfering compounds, using the substances, commonly found in biological fluids (ascorbic and uric acids) and environmental objects (heavy metals Cd^{2+}, Co^{2+}, Cu^{2+}). Pure, non-contaminated control samples were compared to the samples spiked with interfering compounds (see Table 3). The interference for the normal physiological level of the ascorbic acid (50 μM), increased the $MnO_2/(PDDA/PAS)_2$/PDDA/ChOx biosensor response to 394% and decreased to 0.5% at concentration 0.5 μM in the sample spiked with choline. Similar effect was found for the uric acid (see Table 3). Thus, 200-fold dilution of real blood samples is necessary to eliminate the interference of analogous concomitant compounds on studied electrode response.

Heavy metals (Cd^{2+} and Co^{2+}) are reversible inhibitors of choline oxidase [40]. The inhibition effect of Cd^{2+} and Co^{2+} ions is negligible at the concentrations, lower than 10 μM Cd^{2+} and 0.1 mM Co^{2+},

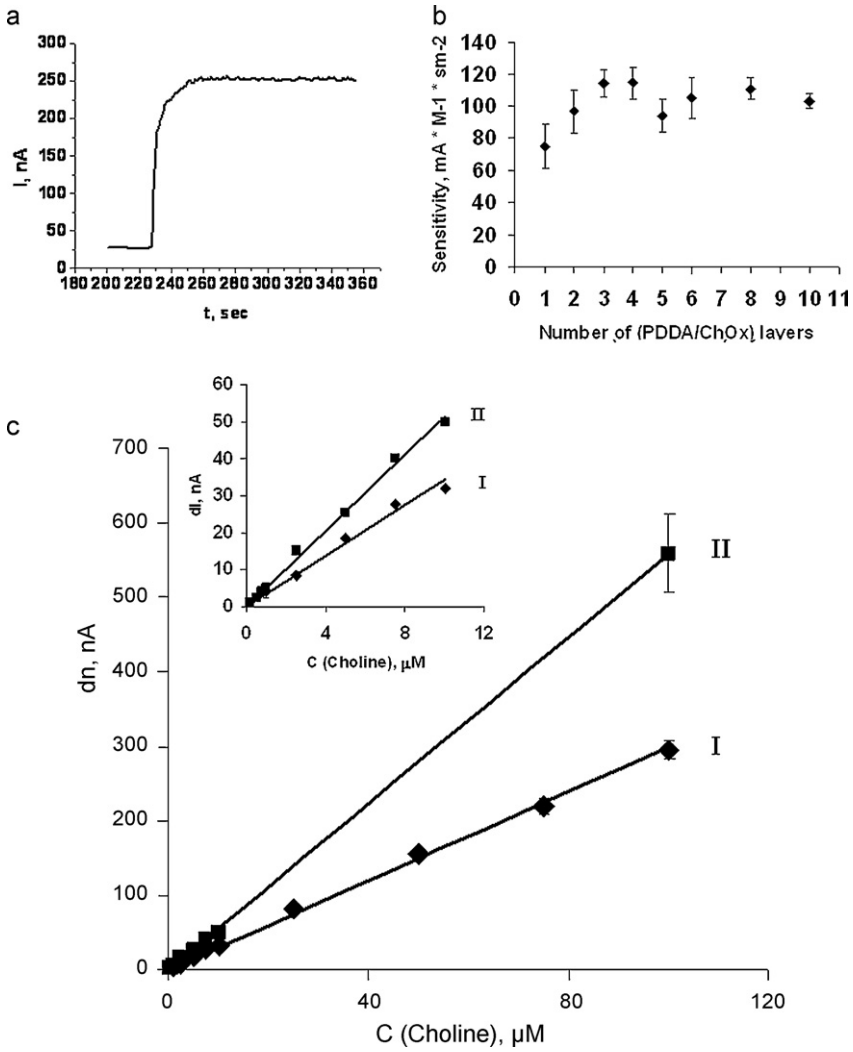

Fig. 9. (a) Analytical response to 0.1 mM of choline and (b) dependence of choline oxidase biosensor sensitivity on number of PDDA/ChO layers and (c) dependence of the MnO_2/(PDDA/PAS)$_2$/PDDA/ChOx (line I) and MnO_2/(PDDA/PAS)$_2$/(PDDA/ChOx)$_3$ (line II) sensors responses at the different concentration of choline. Measurement conditions: 50 mM Hepes, 30 mM KCl, pH 7.5, 480 mV vs. Ag/AgCl.

respectively (Table 3). In our experiments, Cu^{2+} did not influence choline oxidase electrode function, in concentration <1 μM.

3.4. Application of choline oxidase based biosensor

The present study investigates two types of practical applications for the developed choline oxidase electrode MnO_2/(PDDA/PAS)$_2$/(PDDA/ChOx)$_3$. The analysis of blood esterases in biological fluids is important for monitoring of individuals, exposed to cholinergic and/or neuropathic organophosphorus compounds [42]. Fig. 10 demonstrates the results of BChE detection in mice blood haemolysates (200-fold diluted and spiked with enzyme). The corresponding straight lines presented in Fig. 10(a and b), indicate the absence of matrix effect on the biosensor signal. The ordinate shift of the dependence calibration line (Fig. 10(b)), corresponds to the intrinsic enzymatic activity in blood haemolysate samples.

Another important application of the biosensor is the analysis of cholinesterase inhibitors for ecological monitoring and environmental surveillance [43]. It is essential to measure the activity of cholinesterases before and after incubation with inhibitors. Fig. 11(a) shows the calibration curve for BChE detection. The biosensor response is linearly connected with enzyme concentration in the range of 0.005–0.1 nM. The detection limit for BChE,

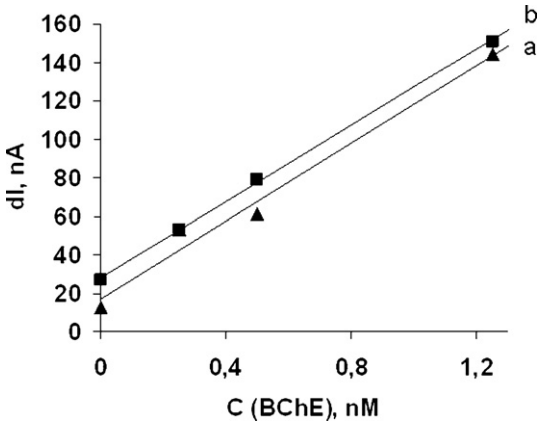

Fig. 10. Biosensor responses at different BChE concentration (a) in 50 mM Hepes, 30 mM KCl and 1 mg ml^{-1} BSA, pH 7.5; (b) in mouse blood sample diluted with Hepes buffer in 200 times after 30 min incubation with 0.01 M butyrylcholine. Measurement conditions: 50 mM Hepes, pH 7.5, 30 mM KCl, 480 mV vs. Ag/AgCl. Slopes: (a) 101 ± 2 nA/nM, (b) 99 ± 1 nA/nM.

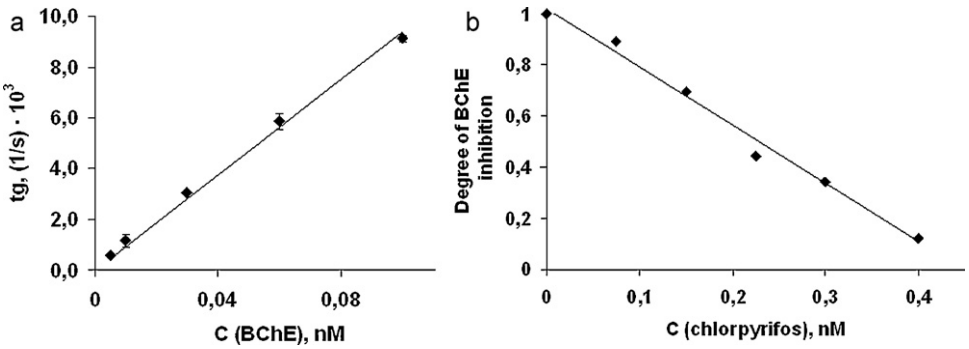

Fig. 11. (a) Biosensor responses at different BChE concentration measured by kinetic method. (b) Degree of BChE inhibition at different chlorpyrifos concentrations. Measurement conditions: Hepes 50 mM pH 7.5 buffer, containing 30 mM KCl 1 mg ml^{-1} BSA at working potential 480 mV (vs. Ag/AgCl reference electrode), 10 min incubation with inhibitor.

Table 3
The effect of interfering compounds on analysis of choline. Electrodes: MnO_2/(PDDA/PAS)$_2$/PDDA/ChOx. Measurement conditions: 50 mM Hepes, pH 7.5, 30 mM KCl, 480 mV vs. Ag/AgCl, choline concentration in the electrochemical cell 0.1 mM.

Components of biological liquids	Normal level in human blood serum [41]	Measured concentration	Response change (%)
Ascorbic acid	50 μM	50 μM	394 ± 12
		5 μM	29 ± 3
		2 μM	13.7 ± 3.3
		0.5 μM	0.5 ± 4.5
Uric acid	500 μM	50 μM	129 ± 47
		5 μM	24 ± 11
		2 μM	−1.0 ± 2.4
		0.5 μM	15 ± 10
Ions of heavy metals	**Maximum permissible concentration in fresh water**	**Measured concentration**	**Response change (%)**
Cd^{2+}	10 mg m^{-3} (90 nM)	1 mM	−40 ± 0
		0.1 mM	−19.5 ± 1.5
		10 μM	−4.5 ± 0.5
Co^{2+}	0.01 mg l^{-1} (170 nM)	1 mM	−26.5 ± 0.5
		0.1 mM	−10 ± 0
		10 μM	−5 ± 0
Cu^{2+}	2 mg l^{-1} (30 μM)	1 mM	−89 ± 4
		10 μM	−40.5 ± 1.5
		1 μM	−6 ± 2

based on the following equation: $y = 2.35x + 0.01$, (where y represents butyrylcholine enzymatic hydrolysis rate and x - the BChE concentration in nM), was estimated as 5×10^{-12} M. Based on the results the developed biosensor is capable of analyzing the degree of BChE inhibition. Fig. 11(b) presents the appropriate degree of BChE inhibition at different chlorpyrifos concentrations. The detection limit for chlorpyrifos was estimated as 5.0×10^{-11} M.

It follows, that the developed biosensor can be used for the detection of cholinesterases and their inhibitors in blood and environmental samples.

4. Conclusion

We have demonstrated the efficiency of γ-phase-MnO_2-based hydrosol, deposited on carbon SPE, as a new transducer element of enzymatic biosensors platforms, fabricated with "layer-by-layer" technology. The detection limit for choline 130 nM, obtained by the developed biosensors, was the lowest in comparison to similar devices reported previously. The revealed analytical characteristics of the choline oxidase biosensor have potential for highly-sensitive monitoring of cholinesterases and their inhibitors in biological and environmental samples.

Acknowledgements

The financial support for this work from Russian Foundation for Basic Research (project no. 10-08-00895-a and 11-08-01306-a) is gratefully acknowledged. The authors are also grateful to Prof. Klyachko N.L. (Department of Chemistry, MSU) for fruitful advice in hydrosol obtaining, Savilov SV (Department of Chemistry, MSU) for characterization of MnO_2 nanoparticles by X-ray diffraction and Amitonov SV. (Physics Department, MSU) for obtaining SEM images.

References

[1] T.L. Rosenberry, Acetylcholinesterase in M. Alton (Ed.), Advances in Enzymology and Related Areas of Molecular Biology, 2006, pp. 103–218.
[2] T.C. Marrs, Toxicology of organophosphate nerve agents, chemical warfare agents , in: T.C. Marrs, R.L. Maynard, F.R. Sidell (Eds.), Toxicology and Treatment, Wiley, New York, 2007, pp. 191–221.
[3] J. Bajgar, Biological monitoring of exposure to nerve agents , Br. J. Ind. Med. 49 (1992) 648–653.
[4] B.W. Wilson, J.D. Henderson, Blood esterase determinations as markers of exposure , Rev. Environ. Contam. Toxicol. 128 (1992) 55–69.
[5] I.N. Kurochkin, A.V. Eremenko, G.F. Makhaeva, L.V. Sigolaeva, G.V. Dubacheva, R.J. Richardson, Multi-strip assay and multimodal biosensors for environmental and medical monitoring of neurotoxicants , in: C. Dishovsky, A. Pivovarov (Eds.), Counteraction to Chemical and Biological Terrorism in the East Europe Countries, NATO Science for Peace and Security, Series A: Chemistry and Biology, Springer, Dordrecht, 2009, pp. 219–229, ISBN 978-90-481-2341-4.
[6] S. Ledru, N. Ruillé, M. Boujtita, One-step screen-printed electrode modified in its bulk with HRP based on direct electron transfer for hydrogen peroxide detection in flow injection mode , Biosens. Bioelectron. 21 (2006) 1591–1598.
[7] E.A. Dontsova, I.A. Budashov, A.V. Eremenko, I.N. Kurochkin, Hydrogen peroxide-sensitive amperometric sensor based on manganese dioxide nanoparticles , Nanotechnologies in Russia 3 (2008) 510–520.
[8] A. Morrin, R.M. Moutloali, A.J. Killard, M.R. Smyth, J. Darkwa, E.I. Iwuoha, Electrocatalytic sensor devices: (I) cyclopentadienylnickel(II) thiolato Schiff base monolayer self-assembled on gold , Talanta 64 (2004) 30–38.
[9] A. Salimi, A. Korani, R. Hallaj, R. Khoshnavazi, H. Hadadzadeh, Immobilization of [Cu(bpy)2]Br2 complex onto a glassy carbon electrode modified with alpha-SiMo12O40(4-) and single walled carbon nanotubes: application to nanomolar detection of hydrogen peroxide and bromate , Anal. Chim. Acta 635 (2009) 63–70.
[10] V.S. Tripathi, V.B. Kandimalla, H. Ju, Amperometric biosensor for hydrogen peroxide based on ferrocene-bovine serum albumin and multiwall carbon nanotube modified ormosil composite , Biosens. Bioelectron. 21 (2006) 1529–1535.
[11] P.N. Mashazi, K.I. Ozoemenab, T. Nyokong, Tetracarboxylic acid cobalt phthalocyanine SAM on gold: potential applications as amperometric sensor for H_2O_2 and fabrication of glucose biosensor , Electrochim. Acta 52 (2006) 177–186.
[12] W. Li, Z. Wang, Ch. Sun, M. Xian, M. Zhao, Fabrication of multilayer films containing horseradish peroxidase and polycation-bearing Os complex by means of electrostatic layer-by-layer adsorption and its application as a hydrogen peroxide sensor , Anal. Chim. Acta 418 (2000) 225–232.
[13] A.A. Karyakin, E.E. Karyakina, Prussian Blue-based 'artificial peroxidase' as a transducer for hydrogen peroxide detection. Application to biosensors , Sens. Actuators B Chem. 57 (1999) 268–273.

[14] A.A. Karyakin, E.A. Puganova, I.A. Budashov, I.N. Kurochkin, E.E. Karyakina, V.A. Levchenko, V.N. Matveyenko, S.D. Varfolomeyev, Prussian blue based nanoelectrode arrays for H_2O_2 detection , Anal. Chem. 76 (2004) 474–478.
[15] F. Ricci, A. Amine, G. Palleschi, D. Moscone, Prussian blue based screen printed biosensors with improved characteristics of long-term lifetime and pH stability , Biosens. Bioelectron. 18 (2003) 165–174.
[16] F. Ricci, G. Palleschi, Sensor and biosensor preparation, optimisation and applications of Prussian Blue modified electrodes , Biosens. Bioelectron. 21 (2005) 389–407.
[17] S. Mannino, M.S. Cosio, S. Ratti, Cobalt(II, III)-oxide chemically modified electrode as amperometric detector in flow injection systems , Electroanalysis 5 (1993) 145–148.
[18] A. Salimi, R. Hallaj, S. Soltanian, H. Mamkhezri, Nanomolar detection of hydrogen peroxide on glassy carbon electrode modified with electrodeposited cobalt oxide nanoparticles , Anal. Chim. Acta 594 (2007) 24–31.
[19] K. Schachl, H. Alemu, K. Kalcher, J. Jeozkova, I. Svancara, K. Vytoras, Amperometric determination of hydrogen peroxide with a manganese dioxide-modified carbon paste electrode using flow injection analysis , Analyst 122 (1997) 985–989.
[20] K. Schachl, H. Alemu, K. Kalcher, H. Moderegger, I. Svancara, K. Vytras, Amperometric determination of hydrogen peroxide with a manganese dioxide film-modified screen printed electrode , Fresenius J. Anal. Chem. 362 (1998) 194–200.
[21] Sh. Yao, Ju. Xua, X. Yi Wang, Ya. Chena, Sh. Xua, Hua, A highly sensitive hydrogen peroxide amperometric sensor based on MnO_2 nanoparticles and dihexadecyl hydrogen phosphate composite film , Anal. Chim. Acta 557 (2006) 78–84.
[22] Sh. Yao, Sh. Yuan, Yu. Xu, Yi. Wang, J. Luo, Sh. Hu, A hydrogen peroxide sensor based on colloidal MnO_2/Na-montmorillonite , Appl. Clay Sci. 33 (2006) 35–42.
[23] J.A. Cox, R.K. Jaworski, Voltammetric reduction and determination of hydrogen peroxide at an electrode modified with a film containing palladium and iridium , Anal. Chem. 61 (1989) 2176–2178.
[24] A. Domenech, J. Alarcon, Determination of hydrogen peroxide using glassy carbon and graphite/polyester composite electrodes modified by vanadium-doped zirconias , Anal. Chim. Acta 452 (2002) 11–22.
[25] H. Shi, Yu. Yang, J. Huang, Z. Zhao, X. Xu, J. Anzai, T. Osa, Q. Chen, Amperometric choline biosensors prepared by layer-by-layer deposition of choline oxidase on the Prussian blue-modified platinum electrode , Talanta 70 (2006) 852–858.
[26] L. Doretti, D. Ferrara, P. Gattolin, S. Lora, Covalently immobilized enzymes on biocompatible polymers for amperometric sensor applications , Biosens. Bioelectron. 11 (1996) 365–373.
[27] K.M. Mitchell, Acetylcholine and choline amperometric enzyme sensors characterized in vitro and in vivo , Anal. Chem. 76 (2004) 1098–1106.
[28] B.-C. Hsieh, K. Matsumoto, T.-J. Cheng, G. Yuu, R.-L. Chen, Choline biosensor constructed with chitinous membrane from soldier crab and its application in measuring cholinesterase inhibitory activities , J. Pharm. Biomed. Anal. 45 (2007) 673–678.
[29] T. Shimomura, T. Itoh, T. Sumiya, F. Mizukami, M. Ono, Amperometric determination of choline with enzyme immobilized in a hybrid mesoporous membrane , Talanta 78 (2009) 217–220.
[30] S. Sen, A. Gulce, H. Gulce, Polyvinylferrocenium modified Pt electrode for the design of amperometric choline and acetylcholine enzyme electrodes , Biosens. Bioelectron. 19 (2004) 1261–1268.
[31] Y.-H. Bai, D. Ying, J.-J. Xu, H.-Y. Chen, Choline biosensors based on a bi-electrocatalytic property of MnO_2 nanoparticles modified electrodes to H_2O_2 , Electrochem. Commun. 9 (2007) 2611–2616.
[32] X. Qina, H. Wang, X. Wang, Sh. Li, Zh. Miao, N. Huang, Q. Chen, Amperometric choline biosensors based on multi-wall carbon nanotubes and layer-by-layer assembly of multilayer films composed of poly(diallyldimethylammonium chloride) and choline oxidase , Mater. Sci. Eng. C 29 (2009) 1453–1457.
[33] M.V. Porus, G.V. Dubacheva, L.V. Sigolaeva, A.V. Eremenko, I.N. Kurochkin, Determination of cholinesterase activities by using bielectrode sensor system , Sensornye Sistemy 22 (2008) 88–95.
[34] P. Calvert, Inkjet printing for materials and devices , Chem. Mater. 13 (2001) 3299–3305.
[35] Y. Lin, X. Cui, L. Li, Low-potential amperometric determination of hydrogen peroxide with a carbon paste electrode modified with nanostructured cryptomelane-type manganese oxides , Electrochem. Commun. 7 (2005) 166–172.
[36] Y.-H. Bai, H. Zhang, J.-J. Xu, H.-Y. Chen, Relationship between nanostructure and electrochemical/biosensing properties of MnO_2 nanomaterials for H_2O_2/choline , J. Phys. Chem. 112 (2008) 18984–18990.
[37] X. Fu, J. Feng, H. Wang, K.M. Ng, Room temperature synthesis of a novel α-MnO_2 hollow structure for aerobic oxidation of benzyl alcohol , Nanotechnology 20 (2009) 375601, doi:10.1088/0957-4484/20/37/375601.
[38] M. Salomäki, P. Tervasmäki, S. Areva, J. Kankare, The Hofmeister anion effect and the growth of polyelectrolyte multilayers , Langmuir 20 (2004) 3679–3683.
[39] T. Fujimoto, Yo. Mizukoshi, Yo. Nagata, Ya. Maeda, R. Oshima, Sonolytical preparation of various types of metal nanoparticles in aqueous solution , Scripta Mater. 44 (2001) 2183–2186.
[40] H. Yamada, N. Mori, Y. Tani, Properties of choline oxidase of cylindrocarpon didymum M-1 , Agric. Biol. Chem. 43 (1979) 2173–2177.
[41] R.K. Murray, D.K. Granner, P.A. Mayes, V.W. Rodwell, Appendix in Harper's Biochemistry , 21st ed., Mir, Moscow, 1993, pp. 367–384.
[42] G.F. Makhaeva, E. Rudakova, N. Boltneva, L.V. Sigolaeva, A.V. Eremenko, I.N. Kurochkin, R.J. Richardson, Blood Esterases as a complex biomarker for exposure to organophosphorus compounds , in: C. Dishovsky, A. Pivovarov (Eds.), Counteraction to Chemical and Biological Terrorism in the East Europe Countries, NATO Science for Peace and Security, Series A: Chemistry and Biology, Springer, Dordrecht, 2009, pp. 177–194, ISBN 978-90-481-2341-4.
[43] S. Andreescu a, J.-L. Marty, Twenty years research in cholinesterase biosensors: from basic research to practical applications , Biomol. Eng. 23 (2006) 1–15.

Biographies

E.A. Dontsova received her MS degree in Chemistry from Lomonosov Moscow State University, Russia, in 2005. Since September, 2005, she has been working towards her Ph.D. degree at the Department of Chemistry in Lomonosov Moscow State University. Her current research interests include electrochemical sensors and biosensors.

Y.S. Zeifman received her MS degree in Chemistry from Lomonosov Moscow State University, Russia in 2010. Her research interests include bioanalytical assays and biosensors.

I.A. Budashov received his MS degree in Biology from Lomonosov Moscow State University, Russia in 1986. In 1998 he obtained his Ph.D. in Biochemistry from the Research Center of Molecular Diagnostics and Therapy, Russia. At present he is the leading specialist in the Institute of Biochemical Physics (Russian Academy of Sciences). His research interests are biochemistry, physical and chemical methods of biology investigations, biosensor systems, and scanning probe microscopy.

A.V. Eremenko received his MS degree in Pharmaceutical Chemistry from the First Moscow Medical Institute, Russia in 1982. In 1986 he obtained his Ph.D. in Biochemistry and Pharmacology from the Institute of Pharmacology, Russian Academy of Medical Sciences, Moscow. At present he is a Senior Researcher at the Department of Biokinetics, A.N. Belozersky Institute of Physico-Chemical Biology, Moscow State University. His main research interests are biosensors for the detection of pharmacological and toxicological compounds, electrochemical analyzers for clinical and environmental applications.

S.L. Kalnov received his MS degree in Biochemistry from Lomonosov Moscow State University, Russia in 1975. In 1980 he obtained his Ph.D. in Biochemistry from Lomonosov Moscow State University, Russia. At present he is Head of the Laboratory of Diagnostics and Prevention Research Institute; Leading Scientist of Emanuel Institute of Biochemical Physics of Russian Academy of Sciences, Moscow.

I.N. Kurochkin received his MS degree in Chemical Enzymology from Lomonosov Moscow State University, Russia in 1979. In 1985 he obtained his Ph.D. in Chemical Kinetics and Catalysis from Lomonosov Moscow State University, Russia. In 2003 he obtained Doctor of Science degree in Chemical Kinetic and Biotechnology at Lomonosov Moscow State University, Russia. At present he is Head of the laboratory of Postgenomic Chemistry, Professor at Chemical Department of Moscow State University, Head of the Department of Physical and Chemical Biology.